

GIS-based colour composites and overlays to delineate heavy metal contamination zones in the shallow alluvial aquifers, Ankaleshwar industrial estate, south Gujarat, India

Suyash Kumar · K. D. Shirke · N. J. Pawar

Received: 6 March 2007 / Accepted: 6 May 2007 / Published online: 22 May 2007
© Springer-Verlag 2007

Abstract In an attempt to delineate heavy metal contamination precincts and to evaluate the extent and degree of toxic levels, besides their possible sources, 38 water samples from Ankaleshwar Industrial Estate, south Gujarat, India were analyzed. By clutching geochemical analyses and GIS-based colour composites areas depicting anomalously high concentration of heavy metals (Mo, Zn, Pb, Ni, Co, Cd, etc.) in the groundwater were revealed. The multicomponent overlays in grey-scale facilitated in identifying situations of heavy metal ‘hot spots’, and lateral protuberances of the contamination plume around defile stretch of the main stream Amla Khadi flowing through the area. The multiple pollution plumes emerging from other parts of the area further coincide with effluent laden streams and small channels indicating industrial establishments as major sources of groundwater contamination. Influential nature of the streams, accelerated infiltration process, high mass influx and shallow groundwater table are the factors conducive for easy access of heavy metals to the phreatic aquifers affecting over 20 km² area. On the basis of *P/U* ratios (concentration of metals in polluted water to unpolluted water), geogenic and anthropogenic sources have been identified. Very high levels of technogenic elements present in the ground water raise concerns about possible migration into food crops, as the area is an important horticultural locale and is highly cultivated.

Keywords GIS · Groundwater contamination · Heavy metals

Introduction

Increasing levels of heavy metals in the environment has attracted the attention of many workers across the globe (Zhang et al. 1999; Matos et al. 2001; Breward 2003). In most of these studies, soil and sediment pollution by heavy metals is the main focus. However, work pertaining to heavy metals in aquatic environment in general and sub-surface aquatic system in particular is sparse. In developing countries like India, the situation is more dismal, as there is hardly any scientific data available on the topic, in spite of rapid industrialization and urbanization over the last few decades. The Ankaleshwar Industrial Estate (AIE) in the western Indian State of Gujarat is characterized by industrial and urban distends reclaiming a large extent of fertile alluvial flood plains of Narmada river. AIE is essentially a chemical domain, which is a part of the industrial ‘Golden Corridor’ housing 171 industrial estates created by the Gujarat Industrial Development Corporation (GIDC). AIE includes an array of chemical, fertilizer, paint, dyes, glass, pharmaceutical and other allied industries, which have impacted the local environment to a great extent. Discovery of hydrocarbons in the area has further hastened the pace of urbanization and industrialization with concomitant increase in environmental problems. Although there is some information generated by the local NGO’s about levels of heavy metals in industrial effluents, there is no scientific data available on the dispersion of metals in the groundwater. This information is imperative as leaching of heavy metal contaminants into the groundwater is a level-headed and significant hazard (Bleeker et al. 2002) and has concerned researchers worldwide (Demirel and Kulege 2005; Demlie and Wohnlich 2006; Gammons and Madison 2006; Pawar and Nikumbh 1999; Rajmohan and Elango 2005; Santos et al. 2002; Weng and Chen 2000). This

S. Kumar · K. D. Shirke · N. J. Pawar (✉)
Department of Geology,
University of Pune,
Pune 411007, India
e-mail: njpawar@unipune.ernet.in

pronounces the demand for the information on heavy metals in the shallow groundwater of AIE, as most of the local population depends on groundwater as their sole source of water supply for drinking and agriculture use besides other activities. The present study was therefore carried out with the objective of investigating chemical composition of both stream and groundwater to (1) determine the extent and degree of toxic metals contamination and (2) delineate areas of heavy metals contamination and their possible sources pictorially by clutching geochemical analyses and GIS-based colour composites.

Study area

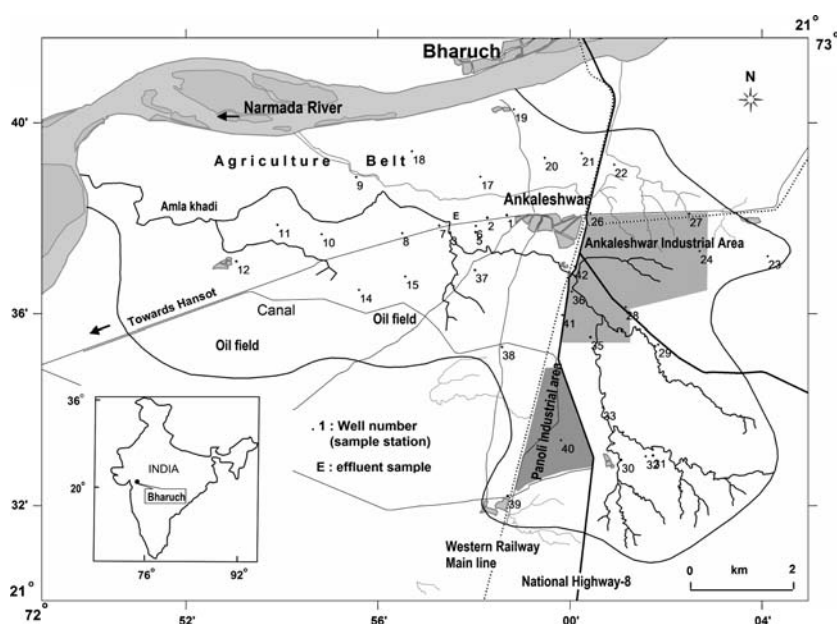
The study area (AIE) is located in Bharuch district of south Gujarat in western India (latitudes $21^{\circ} 30'$ and $21^{\circ} 42'$ and longitudes $72^{\circ} 49'$ and $73^{\circ} 05'$). It is drained by a small third-order stream, Amla Khadi with watershed area of approximately 240 km^2 . Amla Khadi is one of the tributaries of Narmada river that originates in the lower reaches of alluvial flood plain of Narmada (Fig. 1). The area receives an average annual rainfall 860 mm recorded at Bharuch. It is also known for rich agriculture endowed with fine crops of cotton, horticulture and vegetables due to fertile alluvial soils and perennial availability of water. The Amla Khadi stream along its length is divisible into three distinct zones viz. (1) source region with dry stretch, (2) middle ponding segment and (3) lower dry reach. While, the AIE restrains to the upper and middle reaches of the stream, towards lower middle zone in the southwestern part Ankaleshwar oil field is spread over a large area. The lower part of the stream and the areas along the Narmada

riverbanks are known for rich farming where groundwater exploitation is relatively higher. The stream segment in the lower reaches runs foamy red with a pungent foul smell as it carries only industrial effluents with toxic heavy metal concentrations several thousand times the permissible limits. This polluted stretch of Amla Khadi meanders through the agriculture belt with a few isolated industrial establishments on Ankaleshwar–Hansot road. During monsoon the stream overflows submerging the surrounding lands under polluted waters (Santillo et al. 1996). The AIE incorporates two industrial zones: (1) Ankaleshwar industrial area (AIA) and (2) Panoli industrial area (PIA). Both these sectors together comprise over 3,000 industrial units; over half of which are chemicals, manufacturing dyes, paints, fertilizers, pharmaceuticals, industrial chemicals, pulp and paper and pesticides (Bruno 1995; CPCB 1996). Aligned parallel to National Highway No. 8 (Mumbai–New Delhi) and Western Railways, Ankaleshwar is one of the biggest industrial townships in India. The members of the AIE generate between 250 and 270 million liters/day of liquid waste and $\sim 50,000$ tonnes of solid waste annually (Bruno 1995). Of this, 58% arises from the manufacture of dyes and dye intermediates, 19% from drugs and pharmaceuticals, and 5% from inorganic chemicals (CPCB 1996). This set up in the basin provides an ideal site to monitor the interplay between the sources of heavy metals and the response of aqueous system to them.

Geology and hydrogeology

The geology of the area is characterized by Quaternary alluvium. Alluvial sediments have been differentiated on

Fig. 1 Location map of the Ankaleshwar Industrial Estate, South Gujarat, India



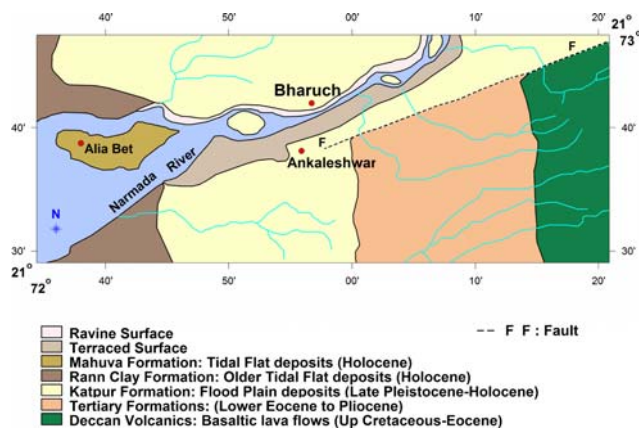


Fig. 2 Regional geological map of the study area (modified after GSI 2002; Chamyal et al. 2002)

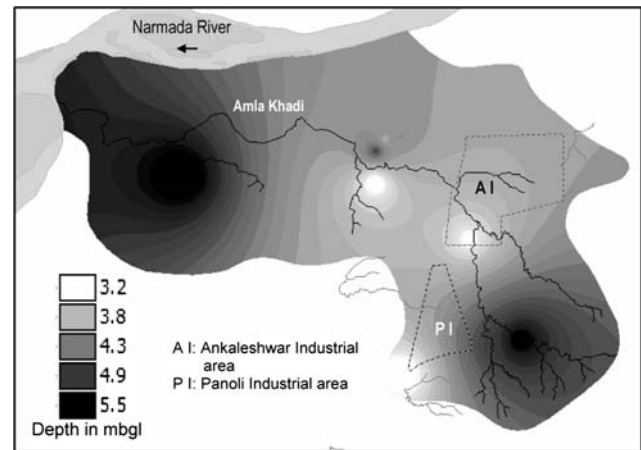


Fig. 3 Depth to water table map of the study area

Table 1 Geological succession in the Ankaleshwar area, south Gujarat, India

Actual depth (m)	Lithology	Age
0–20	Sands, brown clays and gravels, Alluvium	Holocene
20–195	Grey clays, brown clays and gravelly sands.	Recent to Pliocene
195–678	Grey clays, brown clays, shales and sands	Miocene

the basis of their depositional environment by GSI (2002). They comprise older tidal flat and tidal marsh deposits of Rann Clay Formation and younger tidal flat deposits (spit/bar and shoal) of Mahuva Formation, representing marine environment. The flood plain deposits of Katpur Formation represent fluvial environment of deposition (GSI 2002). The AIE belongs to Katpur Formation wherein low-lying flood plain south of Narmada exhibits poorly developed natural drainage and very low relief (Fig. 2). It forms a part of regional alluvial deposits of Late Pleistocene to Holocene in age (Bhandari et al. 2001; Chamyal et al. 2002) through which the stream Amla Khadi drains. The saline wastelands and swampy areas of broad estuarine mouth bar of river Narmada (Alia bet) and older Tidal flat/marsh deposits mark the western boundary of this plain. Towards south and east, the plain is bounded by uplands comprising rocks of Tertiary Sequence (Lower Eocene to Pliocene) and Deccan Volcanics (Chamyal et al. 2002). The topmost subdivision of the alluvial succession, forms host for most of the shallow aquifers in the area (up to 25–30 m depth) and comprises of silty sands, brown to black clays and gravels (Table 1).

The Amla Khadi is a small stream, which along its length shows presence of dry and wet stretches. The uppermost reach is dry (influential in character) except in monsoon. The soils in this stretch are clayey and fine silt dominated, with deeper water table depths (4.9–5.5 mbgl) (Fig. 3). Between PIA and AIA, the stream exhibits natural water flow conditions (effluent in character) with relatively unpolluted surface waters even during peak of the summer in May. Fine sandy soils and sediments with relatively shallow water table depths (3.2–3.8 mbgl) in open wells distinguish this stretch (Fig. 3). The bore wells are sparse and dug well density in this part of the stream is also high (4–6 dug wells/km²). Beyond this ponding middle stretch, in the downstream, the stream carries only effluents released by the industries. Lower reaches portray clayey silt dominated soils and sediments with higher clay content in the top horizons. These clay rich strata are several meters thick at places and act as aquitard. Deeper depth to water levels (>5 mbgl) in dug wells and high density of bore wells (18–20 bore wells/km²) characterize the lower reaches of the stream.

The sand and gravel aquifers in the area are recharged from June to September by the southwest monsoon. On account of rainwater recharge, the unconfined phreatic aquifers in the gently sloping ground towards N–W generate groundwater flow downstream towards Narmada. The availability of groundwater is fairly good throughout the year. The mean static water level in the dug wells during pre monsoon is 4.2 m whereas it is 2.9 m during post-monsoon indicating an average water table fluctuation of 1.3 m. Low lying areas close to river Narmada are waterlogged for more than 2–3 months during monsoon. Small streams and channels in the upper reaches have been targeted for the construction of tanks as water impoundment

measures. These structures have substantially influenced the groundwater levels in the area.

Materials and methods

Since the purpose of the present study was to delineate spatial variations in the toxic metals and to identify their possible sources (industrial/urban, etc.) impacting the subsurface aqueous environment, the sampling plan was designed accordingly. Random sampling technique was adopted for the selection of water sampling wells and due consideration was given to represent industrial, urban and oil field areas besides highways and polluted stream stretches. However, only few samples could be collected from the industrial and oilfield areas due to constraints in the field. Due care was taken to avoid contamination of samples during handling. For every well, separate 1 l capacity polyethylene pre-cleaned containers were used after thoroughly rinsing with the sample water and labeled properly. Operating conditions of well, GPS locations, static water levels, well depths and dimensions, etc. were recorded in the field. Samples from dug wells were collected after the well was subjected to pumping for half an hour. In bore wells fitted with hand pumps or submersibles, samples were collected after pumping the well for few minutes. In all 37 samples from water supply wells (and 1 effluent sample E; Fig. 1) were collected during pre monsoon season (May 2006). Suction filtered (through 0.45 μm membrane filter paper) and acidified samples were employed to determine ten trace constituents by standard addition method (APHA et al. 1985) and using Varian (1275 AA) atomic absorption spectrophotometer (Table 2).

The data (Table 2) were further utilized for generation of geochemical maps in the GIS environment as depicted in flow chart (Fig. 4). The geochemical and spatial data were compiled, merged and loaded in the GIS image processing software ILWIS 3.2 Academic (ITC, RSG/GSD, Jan. 2004). The processed data for ten trace constituents (Fe, Mn, Pb, Zn, Cu, Co, Ni, Cd, Cr and Mo) were used for depicting images of concentrations of individual element, three elements and multiple element combinations.

Single-component images

For generating, processing and editing the images presented in this article, the geochemical point data were interpolated (with a precision of 1), using moving average option, which performs a weighted averaging on point values and returns a raster map as output. In output grided (raster) image for each chemical element, a grid cell (pixel) represented $0^{\circ}00' 00.143''$ in latitude–longitude coordinate system (i.e. approximately 16 m^2 on ground). The grids

were generated using the inverse distance weight function where pixels that fell more than 10,000 m (limiting distance) apart from a sample point were set to null (no value). The single-component images thus generated are given in Fig. 5a–i and show the actual values (concentration in ppb) of the metal under consideration. To enhance the contrast in the images, linear stretching method was employed by which all pixel values in the input map were proportionately stretched between 0 and 255. As 0 is by default displayed in black, and 255 in white, the contrast is better when the image is displayed.

Three-component colour images

The single-component images generated as above were combined together as colour composites to get additional information about the status of the groundwater contamination by metals. This was achieved by allocating a percentile-classified element image to each of the red, green and blue bands. The resulting image uses Red-Green-Blue (RGB) primary colour combination logic, such that red + green = yellow, red + blue = magenta, green + blue = cyan and red + green + blue = white. A wide range of shades was produced depending upon the pixel values of the primary colour shade in the single component image. In the present study, three colour composites comprising Co–Cd–Cr, Pb–Zn–Cu and Mo–Fe–Ni were used to display maps for nine heavy metals in the groundwater samples of the area (Figs. 6, 7, 8). Mn was not used due to insignificant concentrations. The choice of metals in each composite was made on the basis of both similarities and dissimilarities in natural geochemical performance, to enhance the anthropogenic signatures (Breward 2003).

Multi-component overlay

The three-component colour images generated as the above-facilitated display of not more than randomly selected three chemical elements. However, combined corollary of dispersion of all elements can be dexterously demonstrated by overlaying all single component images (with 60% transparency level) in inverse grey scale. The resulting image uses inverse gray scale combination logic such that black (255) + black (255) = black (255) and white (0) + white (0) = white (0), with different intermediate grey shades. This technique conspicuously categorizes and demarcates the zones with high and comparatively low concentrations of metals in the groundwater system (Fig. 9). The significance of this procedure is that as the number of overlays increases, areas of exclusively high anomalies with respect to all components are tainted, and those with comparatively low incongruities are subdued due to multiplicity of grey

Table 2 Trace element data for the groundwater from Ankaleshwar area, south Gujarat, India

Well No.	X (longitude)	Y (latitude)	Mo	Zn	Pb	Ni	Co	Fe	Cd	Cr	Cu
DW 1	72.98	21.63	310	1,458	170	315	287	166	94	43	28
DW 2	72.97	21.63	2,660	944	310	213	243	269	3	1	59
BW 3	72.96	21.63	1,830	698	130	266	287	181	17	1	1
DW 5	72.97	21.63	550	802	170	514	277	282	892	1	18
BW 6	72.97	21.63	2,700	765	240	383	252	257	423	1	1
BW 7	72.95	21.63	1,920	732	260	292	271	250	128	18	1
BW 8	72.94	21.63	1,460	693	250	289	261	256	25	4	1
BW 9	72.93	21.65	2,520	729	240	314	204	195	199	1	55
BW 10	72.91	21.63	2,100	615	260	352	252	223	247	1	46
BW 11	72.90	21.63	2,760	785	430	357	277	306	264	90	1
DW 12	72.88	21.62	1	957	260	310	298	244	100	1	1
BW 14	72.93	21.61	2,250	660	490	463	272	120	578	119	1
BW 15	72.94	21.61	2,640	634	290	369	280	220	151	1	1
BW 17	72.97	21.65	1,380	704	300	415	305	250	429	1	1
BW 18	72.95	21.66	1,950	665	350	378	273	265	313	1	1
BW 19	72.98	21.67	2,130	661	350	473	309	280	520	1	1
BW 20	72.99	21.65	1	1,929	380	395	303	324	294	1	1
BW 21	73.00	21.66	1,990	809	300	290	275	306	2	44	1
BW 22	73.02	21.65	2,310	788	420	352	264	266	218	87	1
BW 23	73.07	21.62	1	5,941	380	295	312	272	17	1	1
BW 24	73.04	21.62	2,440	739	340	356	253	239	271	1	1
BW 26	73.01	21.64	1	1,207	490	318	289	229	55	1	1
BW 27	73.04	21.63	1,080	4,220	460	288	270	160	16	1	1
BW 28	73.02	21.60	1	718	340	345	296	285	184	22	1
BW 29	73.03	21.59	1,400	710	360	285	291	270	11	149	14
DW 30	73.02	21.55	300	722	440	412	299	287	364	1	1
DW 31	73.03	21.55	350	2,477	510	282	298	824	29	1	198
BW 32	73.03	21.55	2,090	695	460	418	282	205	316	1	1
BW 33	73.01	21.57	2,670	714	410	325	315	310	3	42	1
DW 35	73.01	21.59	90	664	490	1	337	318	1	9	30
BW 36	73.01	21.61	1	933	500	230	271	235	1	1	1
DW 37	72.97	21.62	150	596	540	346	317	298	126	44	1
DW 38	72.98	21.59	1,870	589	630	281	289	243	1	1	17
DW 39	72.98	21.54	130	863	520	490	265	240	594	1	1
BW 40	73.00	21.56	2,520	697	380	356	302	264	433	52	1
BW 41	73.00	21.60	2,250	698	680	308	276	290	1	1	5
BW 42	73.00	21.62	2,500	659	430	311	290	265	70	79	16
DW: dug well		Maximum	2,760	5,941	680	514	337	824	892	149	198
BW: bore well		Minimum	1	589	130	1	204	120	1	1	5
		Average	1,440.7	1,077	377.3	334.8	282.2	267.4	199.7	22.3	44.2
Effluent sample (E)	72.96	21.63	88,000	61,410	20,000	43,800	31,200	28,600	29,600	8,100	1

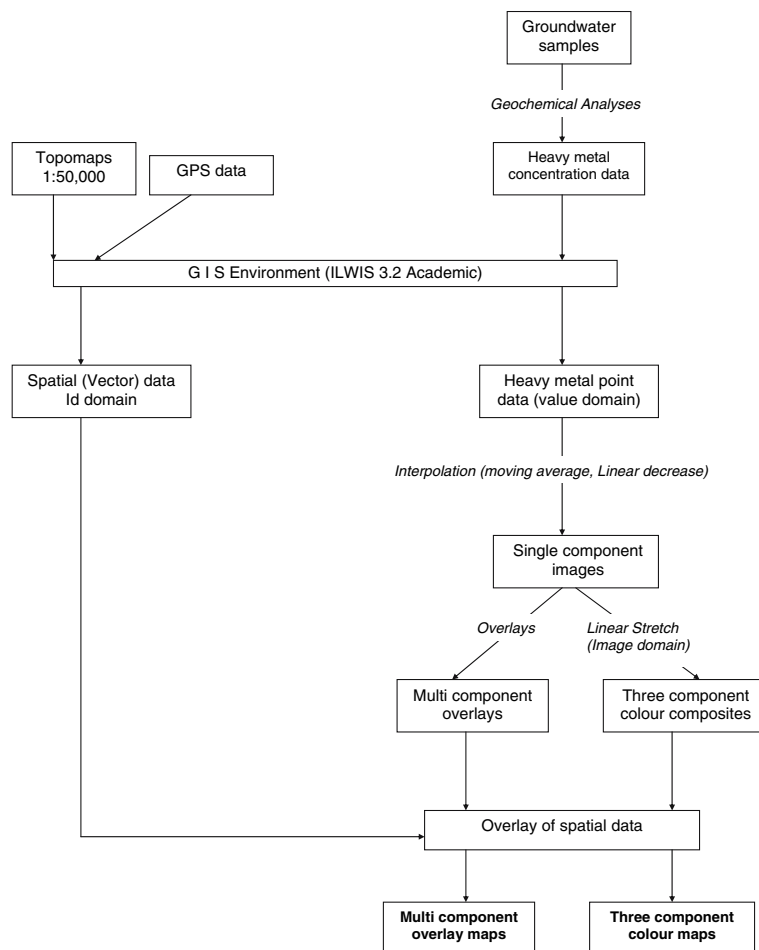
All values are in ppb; 1 denotes not detectable concentration

shades. Therefore, this technique was espoused in identifying hot spots of heavy metal contamination plumes in the groundwater of AIE. The thematic maps engendered by adopting above procedures were used for interpretation and computations.

Results and discussion

The groundwater geochemical attribute coverage of AIE was designed mainly to swathe alluvial flood plain areas reclaimed by industrial, urban, agricultural and oil field

Fig. 4 Flow chart depicting data processing techniques



developments; in order to assess the impact of these activities on the status of groundwater in the context of toxic trace elements. As the area is poorly drained, the content of metal species is expected to be relatively high. The extent and very high concentrations of heavy metals particularly Mo, Zn, Pb, Ni, Co, Fe and Cd (in decreasing hierarchy of abundance) perceived in the analyses were far in excess from those expected (Table 2).

Spatial dispersion of heavy metal species

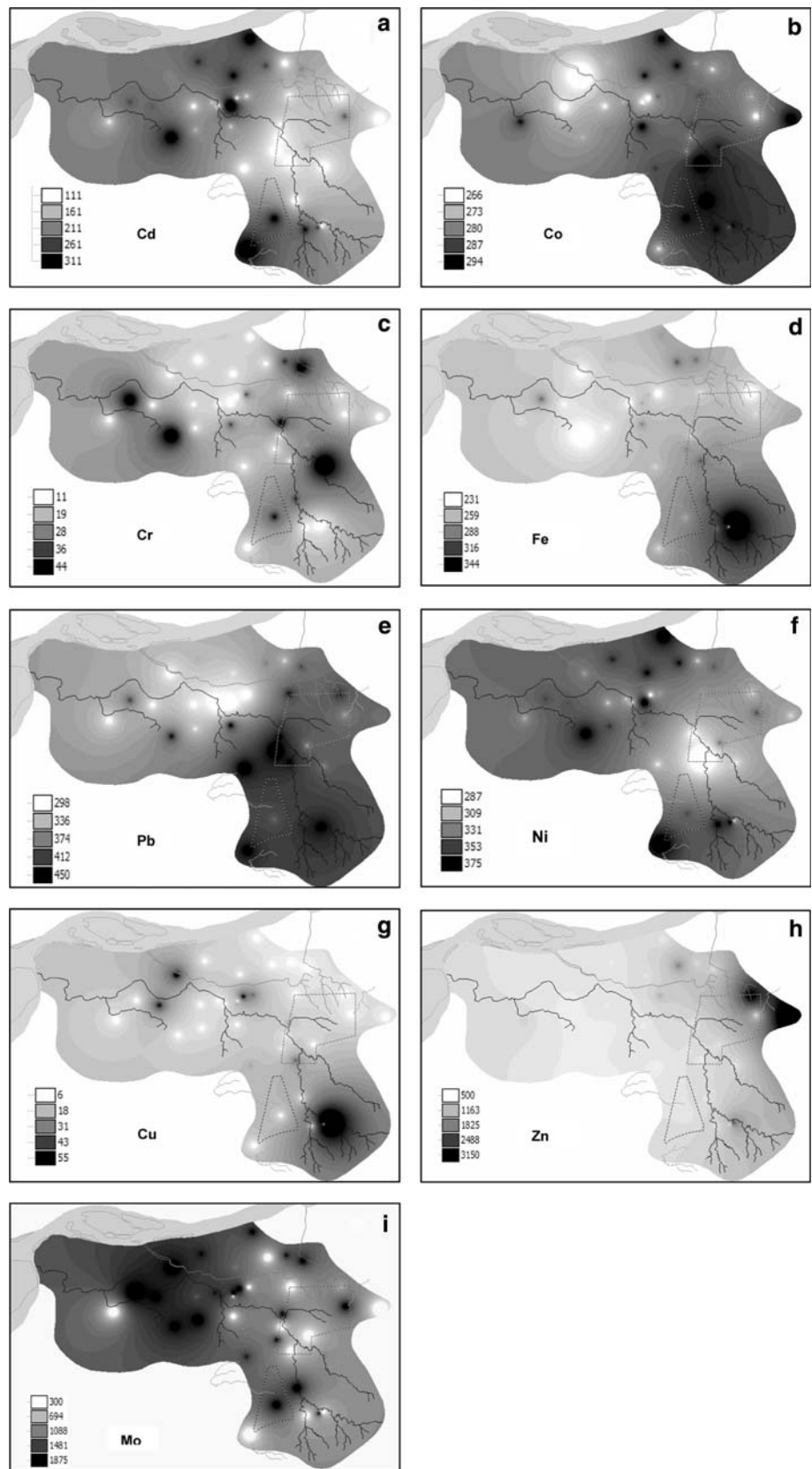
The single-component images (Fig. 5a–i) unveil the spatial dispersion of heavy metals in the groundwater of Ankaleshwar area. In spite of the fact that the catchment region of Amla Khadi is bounded by Deccan volcanics in the east and south, notably low levels of chromium (average 22 ppb in 37 wells) were recorded. This implies that the surface alluvial sediments (in which nearly all aquifers subsist) are derived from Cr deficient (low-Mg, tholeiitic) lava flows from Deccan Volcanic Province (Beane et al. 1986). However, very high concentration of Cr (8,100 ppb) in the surface water sample (E) from effluent laden stretch of

Amla Khadi (Table 2) authenticates its anthropogenic source particularly from the Industry. In this stretch, stream carries only industrial wastes. The same holds true for other metals also except copper (Table 2). Lower concentration levels of Cu delegate towards absence of both lithogenic and anthropogenic sources in the catchment areas.

High concentrations of chromium (in limited wells and the effluent sample) could be from tanneries, pharmaceuticals, pigments, metal works or a combination of all, whereas possible sources of cadmium could range from non-point sources such as application of phosphate fertilizers to point sources including pigment and metal works (Demlie and Wohnlich 2006). Pigments and pharmaceuticals are major industries in the study area and hence could contribute to Cr in some instances. Similarly the Cd concentrations are also higher indicating its likely source related to industries. Both the metals are highly toxic and can be easily taken up and accumulated by plants and crops through the root systems (Alam et al. 2003).

Lead has long been recognized as an industrial hazard (Krishna and Govil 2004). Elevated concentrations of Pb may be attributed to fertilizer and paint industries. How-

Fig. 5 a–i Single component images of the study area (index values in ppb)



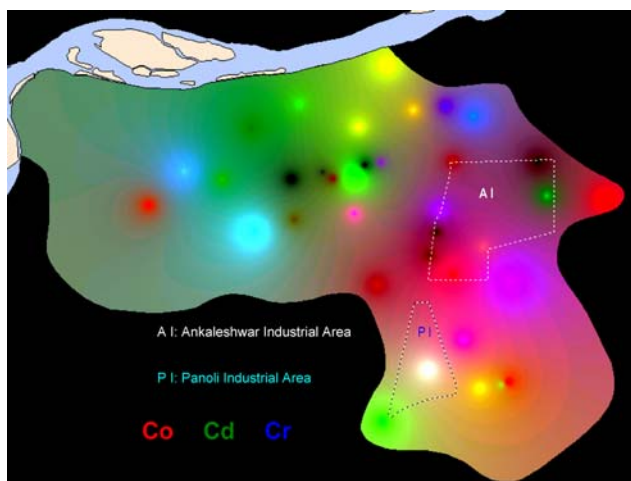


Fig. 6 Three-component color composite of the study area (Co–Cd–Cr)

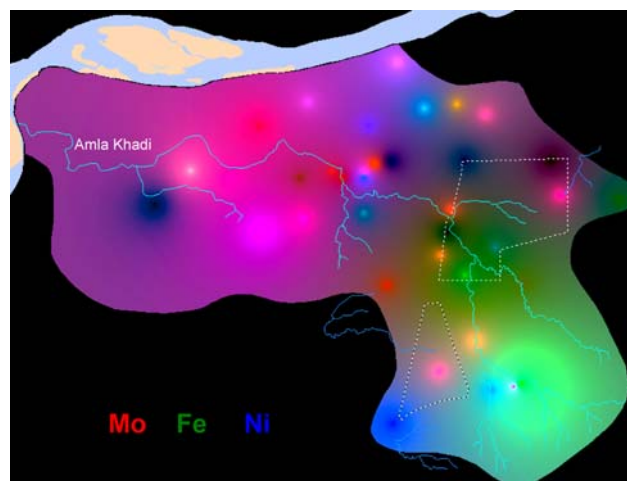


Fig. 8 Three-component color composite of the study area (Mo–Fe–Ni)

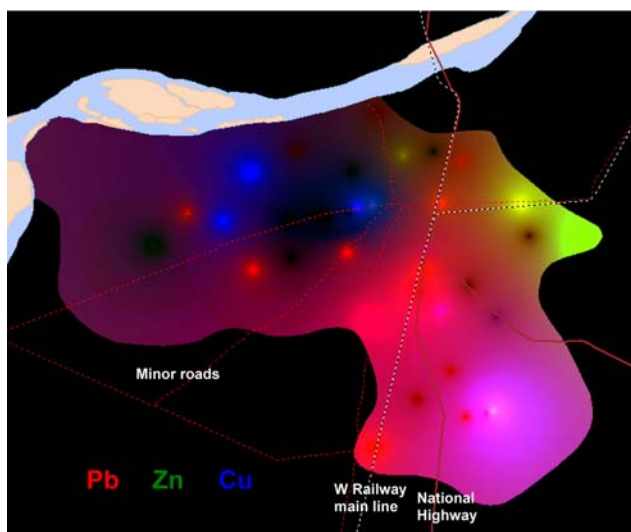


Fig. 7 Three-component color composite of the study area (Pb–Zn–Cu)

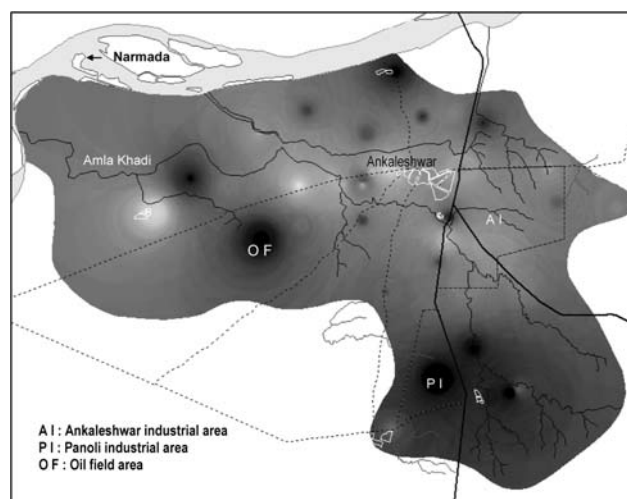


Fig. 9 Multi-component overlay depicting multiple heavy metal hotspots in the study Area

ever, higher dispersion of Pb in the groundwater of AIE and areas adjoining highways, points towards highway environment as a major source of the metal (Harrison et al. 1981). This is more evident in the three-component (Pb–Zn–Cu) colour composite (Fig. 7).

Cobalt, nickel, zinc and molybdenum are present in almost all wells with abnormally high concentrations in a few. Source of Co in the environment could be the burning of coal and the industrial processes that use the metal or its compounds (Krishna and Govil 2005). Coincidentally the dispersion pattern of high Co is confined to the industrial areas where burning of coal is a major source for energy (Fig. 5b).

Nickel is known for its considerable spatial variation in the soils, even on a small scale (Proctor and Baker 1994) and also for its temporal variability, which is not typical of heavy metals (Xiangdong et al. 2004). However, it does not show significant spatial variation in the groundwater of the area under review (minimum 213, maximum 514 ppb with one exception). High nickel concentrations are also connected to morphogenetic characteristics of the greater region; primarily the basic rocks. One of the possible geogenic sources of Ni could be from weathering of pyroxenes (augite) from basalts (Beane et al. 1986). However, high concentrations of this metal in the effluent sample (43,800 ppb) are allied to substantial anthropogenic input particularly from battery wastages in garbage dumps and also from petroleum filling tanks (Demirel 2006). The Fe

(minimum 120, maximum 324 and effluent sample 28,600 ppb) values in groundwater from the study area are also partly attributable to above sources as well as petroleum and water distribution pipelines (Demirel 2006).

Although the average concentration of zinc is less than that of molybdenum, its high concentrations at all the wells (minimum 589, maximum 5,941 ppb) and highest values in the eastern fringes of AIE reflect significant contributions from industries. Widespread dispersion of zinc could be attributable to the use of liquid manure, decomposed materials and agrochemicals (Krishna and Govil 2005). This is supported by the least concentration of Zn viewed in the oil field areas where agriculture is not a major activity (Fig. 5h).

Molybdenum is essential for all life forms and in plant nutrition that helps in nitrogen fixation and other metabolic processes. Significant usage of this metal is made as refractory metal in numerous chemical applications including catalyst in oil refinery, oil pipelines and lubricants besides as pigments in paints and inks (Demirel 2006). Widespread dispersion of Mo all over the area (Fig. 5i), its high concentrations in oil field area and extremely high concentrations in effluents suggest a multi-source contribution of this element including modern agronomic practices, industries and oil field developments.

Ankaleshwar is an important agriculture and horticulture center that has encouraged significant contributions from widespread use of micronutrient fertilizers and pesticides. The trace elements from these sources have possibly been added to the aquifers (Pawar and Nikumbh, 1999, Romic and Romic 2003). This is supported by the uniform and high-level spatial distribution of Zn and Mo, which are important constituents of micronutrient fertilizers.

Local technogenic anomalies

In the Co–Cd–Cr (RGB) composite (Fig. 6), two distinct zones have been observed. The industrial zone (consisting of AIA and PIA) is marked by a red (Co)-magenta (Co–Cr) hue, in contrast to the green (Cd)-cyan (Cd–Cr) hue in other parts. A conspicuous white anomaly in the core part of the Panoli industrial area is evident where all the three bands have maximum (255) values, representing ‘all high’ concentrations of the ingredient metals. Cyan (Cd–Cr) anomaly in the oil field area, magenta (Co–Cr) and yellow (Co–Cd) around industrial areas, are clearly visible.

The Pb–Zn–Cu composite (Fig. 7) illustrates exceedingly skewed image wherein the red band (Pb) ‘stands out’ and is huddled around major highway (National Highway No. 8) and rail route (Western Railway main line). This is in conformity with many earlier studies (notably Harrison et al. 1981; Laxen and Harrison 1977), specifying traffic emissions as a major contamination source of the metal.

The dark misty areas represent relatively unsullied zones with respect to these metals and indicate a possibly shrinking pollution plume due to discontinued usage of leaded petrol. The green (Zn) hue lies in the eastern fringes of Ankaleshwar Industrial area confirming primary anthropogenic inputs. However, magenta colour cluster (Pb–Cu) on the eastern fringes of Panoli industrial area and sporadic blue bulges (Cu) in the image cannot be considered as anomalies as concentration of Cu is almost insignificant in most of the well water samples.

The Mo–Fe–Ni composite shows abundance of Mo in the downstream aligned with watercourses and intermittent anomalies reliant to their relative concentration. The industrial precinct coincides with dominance of green hue (Ni) that gradually converts through blue into a red/magenta hue downstream in agricultural belt. However, this composite has limitations in revealing the dispersion of Fe from natural and anthropogenic complement because of merging background signals. This is evidenced by diminutive variation in the Fe content in all 37 water samples (minimum 120, maximum 324 with one exception 824 ppb).

Heavy metal hot spots

The multicomponent overlay in inverse grey scale (Fig. 9) depicts heavy metal dispersion and its ultimate abundance in totality. It shows consistent and tightly defined multiple heavy metal ‘hot spots’ spread over the entire study area. Relatively higher dispersion of heavy metals in the ground waters of Panoli industrial area and adjoining situations (darker shades) as compared to the Ankaleshwar industrial area is perceived. This is on account of industrial source located in recharge zone where the conditions are more conducive for mass influx of pollutants in the local hydrologic/aquifer system. Akin to all three-colour composites it shows a conspicuous and dark hot spot in the core sector of the Panoli industrial area. Anomaly near the western fringes of the Ankaleshwar city is at the triple junction of the highway, industrial area and urban center. At this point the polluted stretch of the Amla Khadi stream is also instigated. Two hot spots further downstream and on the banks of Amla Khadi are well marked. Large hot spot (at the southern bank and) in the lower reaches of Amla Khadi represent the pinnacle of the groundwater contamination plume due to polluted stream. Sporadic hot spot anomalies, four on the northern extremity of the area and one on the southwest part of it, are visible. While the northern anomalies fall in the extended Ankaleshwar industrial area coinciding broadly with small watercourses carrying industrial effluents, the other with superior dimensions represents the wedge of the Ankaleshwar oil field. This anomaly representing ‘all high’ is noticeably

Table 3 Areal extent, sites and likely sources of heavy metal hotspots (location in lat. long.; deg min s)

Location of hot spot (centre)	Vicinity	Area (km ²) approx.	Likely source
1: 21 37 51; 72 53 53	Amla Khadi (polluted stretch) downstream	4	Polluted stream
2: 21 36 31; 72 55 34	Oilfield area	7	Oil field developments
3: 21 37 44; 72 58 00	Amla Khadi northern bank (polluted stretch)	4	Polluted stream
4: 21 36 55; 72 58 01	Amla Khadi southern bank (polluted stretch)	0.2	Polluted stream
5: 21 36 59; 73 00 05	Triple junction of industrial, urban area and polluted stream,	1	Industry, urban centre and polluted stream
6: 21 35 57; 72 59 50	Ankaleshwar industrial area	0.2	Industry
7: 21 37 18; 73 02 42	Ankaleshwar industrial area	0.5	Industry
8: 21 33 20; 72 59 47	Panoli industrial area	2	Industry
9: 21 34 04; 73 00 38	Panoli industrial area	1	Industry
10: 21 39 23; 72 56 43	Adjacent effluent laden local streams	0.2	Polluted local stream
11: 21 38 50; 72 58 10	Adjacent effluent laden local streams	0.5	Polluted local stream
12: 21 39 14; 72 59 28	Adjacent effluent laden local streams	0.5	Polluted local stream
13: 21 39 06; 73 00 55	Adjacent effluent laden local streams	1	Polluted local stream

Table 4 Ratios of different metal concentrations in samples from two stretches of Amla Khadi (*P/U*), Ankaleshwar area, South Gujarat, India

Concentration	Mo	Cr	Cd	Ni	Fe	Co	Zn	Pb	Cu
Polluted stretch (<i>P</i>)	88,000	8,100	29,600	43,800	28,600	31,200	61,410	20,000	1
Unpolluted stretch (<i>U</i>)	1	1	101	332	275	319	677	400	1
Ratio <i>P/U</i> (polluted/unpolluted stretch)	88,000	8,100	293	132	104	98	91	50	1

All values are in ppb; 1 denotes not detectable concentration

visible in all three-component colour composites also, and is buttressed with the field verification. It is to be noted that the confines of oil fields, industrial and urban landuse were marked on older topomaps, and these areas have bulged out over the years; the reason for spotting anomalies neighbouring the Panoli industrial area.

Dimensional appraisal, vicinity and likely sources of heavy metal hot spots

As georegistering is an essential prerequisite for data processing in ILWIS, spatial information could be precisely mapped and scaled on the output colour composites and overlays. Multicomponent image in inverse gray scale was used to ascertain the areal extent and sites of contamination plumes for multiple metal combinations depicted as heavy metal hotspots in the study area. Table 3 depicts that the streams and local channels laden with industrial wastes have significantly contributed towards contaminating the shallow aquifers. It is observed from the

table that over 20 km² area has been severely affected by polluted groundwater in the area.

Impact of polluted stream on shallow groundwater

The multicomponent overlay in inverse grey scale is also commendable in evaluating the role of polluted stretch of the Amla Khadi and other grimy streams as potential secondary polluting sources. This is because most of the watercourses in the area are losing streams with no base flow under natural conditions favouring infiltration of metal pollutants into the underlying shallow aquifer system (Pawar et al. 1998). Considering the average concentration of metals in the samples from the unpolluted stretch of the stream Amla Khadi as background (predominantly geogenic) values (*U*), the presumption that—the atypically high concentration of metals in the polluted stretch of the stream (*P*) is anthropogenic—seems to be inescapable. The *P/U* ratio of concentration of different metals in samples from two stretches (polluted and unpolluted) is given in Table 4.

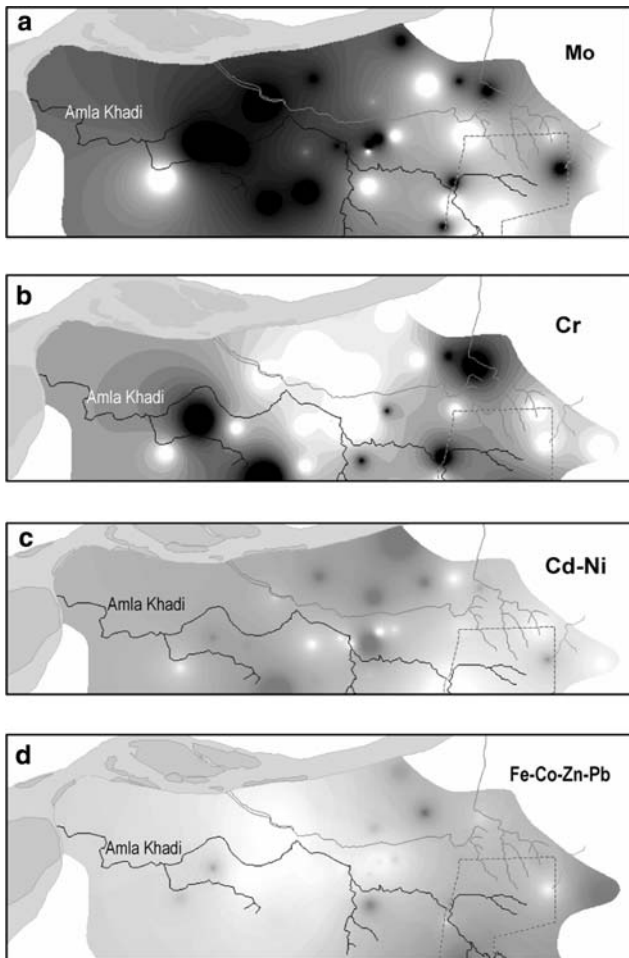


Fig. 10 a–d Extension of contamination plumes around polluted stretch of the streams flowing through the study area

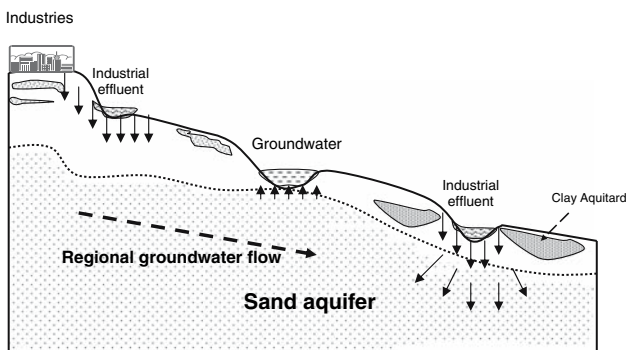


Fig. 11 Geoenvironmental features and movement of heavy metals

It is apparent from Table 4 that the *P/U* ratio is ‘extremely’ high for Mo (88,000), ‘high’ for Cr (8,100), and is ‘low’ for Cd (293), Ni, Fe, Co, Zn and Pb (50). Since, in a single-component image the contamination plume cannot be taken as ‘anomaly’, care was taken while overlaying. It was monitored that high (255) of one image

is not annulled by low (0) of superimposed image; and *P/U* ratio is functional for this intent. For example, the *P/U* ratio for Pb, Zn, Co and Fe is low and these metals show relatively less contaminated zones around entire polluted stretch of the stream. Conversely, this ratio for Mo is extremely high (88,000), and it displays large areas of contamination around entire polluted stretch downstream. Overlays of these images in inverse gray scale invalidate each other without showing any signatures of effluence around the polluted stretch. Therefore, four images (Fig. 10a–d) in inverse gray scale (with 70% transparency level) viz.: Mo (extremely high *P/U* ratio), Cr (high *P/U* ratio), Cd–Ni, and Fe–Co–Zn–Pb (low *P/U* ratio) are presented here, wherein dark shaded areas on either banks along the polluted stretch of the streams, depict the extension of the contamination plume. Because this ratio for Cu is 1, the single component image of Cu was not superimposed in the overlay.

It is observed from Fig. 10a, that the contamination plumes of Mo are intermittently situated throughout the polluted stretch of the streams and have bulged out in the downstream area. However, those of Cr (Fig. 10b) and Cd–Ni (Fig. 10c) are positioned at different situations around this stretch. A diminutive plume in the middle reaches of the stream represents combined consequence of Fe–Co–Zn–Pb (Fig. 10d). Despite the fact that the absolute concentrations of all heavy metal species in the effluent sample is very high (Table 2), disparity in the situations of the plumes depends the varying mobility of these metals in aqueous environment (Mo > Cr > Cd–Ni > Fe–Co–Zn–Pb) and aquifer heterogeneities. However, it should be stated here, that all single-component images used in this article have been derived from a rather coarse input data set due to field constrains, and the statistics at a finer grid interval with additional field verifications could generate more refined images with higher resolutions.

Geoenvironmental controls over groundwater pollution plumes

Geoenvironmental conditions of the area manifestly influence the mechanism of groundwater pollution (Pawar et al. 1998). It is observed that the location of Panoli industrial area in the recharge zone is accountable for more dispersion of heavy metals in the adjoining areas. Heavy metal mounds derived from the waste dumps and effluents from industries are stored in the topsoils throughout the year. Deeper depths of water table and influent (loosing) nature of the streams in this area have accelerated the infiltration process particularly during post-monsoon period when the mass influx is high and the groundwater table is elevated. This has provided easy access of heavy metals to the shallow aquifers in these areas. Ankaleshwar industrial

area is positioned in the middle-lower reaches of the stream. This area has relatively shallower water table depths and the hydrological characteristic of the stream is effluent (gaining) in nature (Fig. 3). Although porous sandy sequences in this stream stretch are favorable for downward percolation of metals, the geoenvironmental conditions are responsible for moderately retarding the diffusion of metals in these areas. Several meter thick clay dominated sequences prevail in the lower reaches of the Amla Khadi. These clay rich sequences function as the ultimate sink for the heavy metals derived from surface sheet flows and streams carrying industrial liquid wastes; and prevent entry of pollutants in the aquifers during dry season when water table is located comparatively at deeper depths (Fig. 11). However, subsequent to monsoon season, the higher levels of groundwater are in direct hydraulic contact with the surface sources of pollution such as clay sinks, sheet flows and effluent carrying stream stretches (as is evidenced by nearly waterlogged conditions in the downstream reaches after wet spell) favouring induced infiltration of metals. Furthermore, areas around the lower reaches of the stream are highly cultivated by means of higher withdrawals of groundwater. In effect, the effluent from the stream as well as heavy metals from the clay sinks are drawn into the aquifers rapidly in these areas; thereby allowing the pollution plume to expand. It needs to be mentioned here that the degree of dilution of polluted water is governed by the base flow conditions of the stream (Blair 1972); however, for most of the times there is no base flow in the Amla Khadi as well as other local streams, except during rainfall events. These geoenvironmental features are the main reasons for the metal pollutants in the unsaturated zone forming a plume of pollution in the saturated zone. Most of the contamination plumes and hot spots located around the watercourses provide strong evidence to this.

Conclusions

The geochemical statistics of heavy metals in the groundwater of Ankaleshwar industrial estate, although, of restricted regional extent, provides a unique data set of substantial interest as it has severe environmental implications from food security and human health point of view. Heavy metal contamination by single or multiple species is observed in almost all water supply wells of the study area. Location of PIA in the recharge zone of the Amla Khadi basin (upper reaches) could be one of the main reasons for higher dispersal of heavy metals in the groundwater. Considering highway environment as the prime source for lead pollution, the decreasing hierarchy of abundance of seven metals in 37 groundwater samples ($\text{Mo} > \text{Zn} > \text{Ni} > \text{Co} > \text{Fe} > \text{Cd} > \text{Cr}$) is exceedingly comparable to

that in the industrial effluents ($\text{Mo} > \text{Zn} > \text{Ni} > \text{Co} > \text{Cd} > \text{Fe} > \text{Cr}$). This strongly points towards the industries as the major primary perpetrator for groundwater pollution in the region. This is evidenced by the presence of multiple heavy metal hotspots in and around industrial areas on the multicomponent overlay. Except Co, Fe, Cu and Zn, all other metals are dispersed in the groundwater of oil field area with alarming concentrations; and the high amplitude hot spot in this area holds the oil field developments accountable for mutilating the subsurface aqueous environment to a regional extent. Computations reveal that over 20 km² area has been severely affected by polluted groundwater in the region. Although there are no significant groundwater withdrawals in the oil field area due to adequate municipal water supply, it would be useful to pierce a few bore wells for characterization of the pollution plume.

Contamination plumes on the multicomponent overlays around the 25 km long defile stretch of the Amla Khadi and other local channels reveal that the stream polluted by industrial sources contrives as a potential secondary source of pollution. The extent and situations of plumes around the tainted stretches of the streams throw light on the varying mobility of metals in aqueous environment. It is ironical that industrial areas detain the recharge zone of the basin and the discharge zone is influenced with exceptionally high levels of toxic effluents; both factors exceedingly damaging the entire shallow subsurface aquatic ecosystem. The strewn hotspots on the multi component overlay imply towards multisource derivation of technogenic elements as well as the aquifer heterogeneities imparted by distribution of clay lenses. The geoenvironmental conditions have largely controlled the movement and dispersion of heavy metals in groundwaters of the Amla Khadi basin. Though, the mechanisms governing bioavailability and phyto-accumulation of heavy metals are not yet fully understood, their antipathetic behaviour with biomass is experienced by the local farmers in the form of decreasing crop yield per hectare over the years, particularly around the polluted stretch of the Amla Khadi stream. Proximity of the area to the coast, and discharge of toxic industrial wastes into it with a measured rate of ~1,190 l/s during peak summer (pre-monsoon), poses further threat to the marine aquatic life, which in turn may enter the food chain and eventually result in health disorders in humans.

Presence of elevated levels of potentially toxic metals in groundwater of the study area implies their high content in the soil resources as well. It must be stressed that as soil characteristics play a key role in movement, storage, and distribution of trace constituents in the groundwater, soil dispositions in the area need further investigations. Nevertheless, value and importance of existent geochemical data and GIS ambiance in identifying quarters of

contaminated subsurface aqueous environment is evidently discernible.

Acknowledgements Authors would like to thank the Head, Department of Geology, University of Pune, for providing necessary facilities. Financial assistance to K. D. Shirke (JRF) by DST and Teachers' Fellowship to Suyash Kumar by UGC is gratefully acknowledged. Help in the fieldwork by Mr. J. B. Pawar and Mr. S. K. Gaikwad is thankfully acknowledged. Thanks are also due to Mrs. Ashwini Supekar for assistance in the analyses of water samples. This study is a part of the DST project under SSS program. The authors gratefully acknowledge the financial support by DST, Government of India. Authors gratefully acknowledge the anonymous reviewers for many meaningful suggestions.

References

- Alam MGM, Snow ET, Tanaka A (2003) Arsenic and heavy metal contamination of vegetables grown in Samta village, Bangladesh. *Sci Total Environ* 308:83–96
- APHA, AWWA, WPCF (1985) Standard methods for the examination of water and waste water, 14th edn. American Public Health Association, Washington, DC, p 1193
- Beane JE, Turner CA, Hooper PR, Subbarao KV, Walsh JN (1986) Stratigraphy, composition and form of the Deccan Basalts, Western Ghats, India. *Bull Volcano* 48:61–83
- Bhandari S, Rachna Raj, Maurya DM, Chamyal LS (2001) Formation and erosion of Holocene alluvial fans along the Narmada-Son Fault around Rajpipla in the lower Narmada Basin, Western India. *J Geol Soc India* 58:519–531
- Blair H (1972) Hydrogeological factors in groundwater pollution. The water Research Association, Medmenham Bucks, UK
- Bleeker PM, Assuncao AGL, Teiga PM, Koe TD, Verkleij JAC (2002) Revegetation of the acidic, as contaminated Jales mine spoil tips using a combination of spoil amendments and tolerant grasses. *Sci Total Environ* 300:1–13
- Breward N (2003) Heavy-metal contaminated soils associated with drained fenland in Lancashire, England, UK, revealed by BGS Soil Geochemical Survey. *Appl Geochem* 18:1663–1670
- Bruno K (1995) Chemical pollution: Gujarat's toxic corridor. *Hindu Soc Environ* 29(9):163–166
- Chamyal LS, Maurya DM, Bhandari S, Rachna Raj (2002) Late quaternary geomorphic evolution of the lower Narmada valley, Western India; implications for neotectonic activity along the Narmada-Son fault. *Geomorphology* 46:177–202
- CPCB (1996) Inventorisation of hazardous waste generation in five districts (Ahmedabad, Vadodara, Bharuch, Surat, and Valsad) of Gujarat. Central Pollution Control Board (Ministry of Environment and Forests, Government of India) ISBN 8186396632
- Demirel Z, Kulege K (2005) Monitoring of spatial and temporal hydrochemical changes in groundwater under the contaminating effects of anthropogenic activities in Mersin region, Turkey. *Environ Monit Assess* 101:129–145
- Demirel Z (2006) Monitoring of heavy metal pollution of groundwater in a phreatic aquifer in Mersin—Turkey. *Environ Monit Assess*. doi 10.1007/s10661-006-9498-9
- Demlie M, Wohnlich S (2006) Soil and groundwater pollution of an urban catchment by trace metals: case study of the Addis Ababa region, central Ethiopia. *Environ Geol* 51:421–43
- Gammons CH, Madison JP (2006) Contaminated alluvial groundwater in the Butte Summit Valley. *Mine Water Environ* 25:124–129
- GSI (2002) District resource map. Bharuch District, Gujarat
- Harrison RM, Laxen DPH, Wilson SJ (1981) Chemical associations of lead, cadmium, copper, and zinc in street dusts and roadside soils. *Environ Sci Technol* 15:1378–1383
- Krishna AK, Govil PK (2005) Heavy metal distribution and contamination in soils of Thane–Belapur industrial development area, Mumbai, Western India. *Environ Geol* 47:1054–1061
- Krishna AK, Govil PK (2004) Heavy metal contamination of soil around Pali Industrial Area, Rajasthan, India. *Environ Geol* 47:38–44
- Laxen DPH, Harrison RM (1977) The highway as a source of water pollution: an appraisal with the heavy metal lead. *Water Res* 11:1–11
- Matos de AT, Fontes MPF, Costa da LM, Martinez MA (2001) Mobility of heavy metals as related to soil chemical and mineralogical characteristics of Brazilian soils. *Environ Pollut* 111:429–435
- Pawar NJ, Nikumbh JD (1999) Trace element geochemistry of groundwaters from Behedi basin, Nasik district, Maharashtra. *J Geol Soc India* 54:501–514
- Pawar NJ, Pondhe GM, Patil SF (1998) Groundwater pollution due to sugar-mill effluent, at Sonai, Maharashtra, India. *Environ Geol* 34:151–158
- Proctor J, Baker AJM (1994) The importance of nickel for plant growth in ultramafic (serpentine) soils. In: Ross SM (ed) Toxic metals in soil-plant system. Wiley, New York, pp 417–432
- Rajmohan N, Elango L (2005) Distribution of iron, manganese, zinc and atrazine in groundwater in parts of Palar and Cheyyar River basins, South India. *Environ Monit Assess* 107:115–131
- Romic M, Romic D (2003) Heavy metals distribution in agricultural topsoils in urban area. *Environ Geol* 43:795–805
- Santillo D, Stephenson A, Labunskaja I, Siddorn J (1996) A preliminary survey of waste management practices in the chemical industrial sector in India: consequences for environmental quality and human health. Part I. Gujarat. Greenpeace Research Laboratories Technical Note 96/8
- Santos A, Alonso E, Callejon M, Jimenez JC (2002) Distribution of Zn, Cd, Pb, and Cu metals in groundwater of the Guadiamar River basin. *Water Air Soil Pollut* 134:275–286
- Weng H, Chen X (2000) Impact of polluted canal water on adjacent soil and groundwater systems. *Environ Geol* 39:945–950
- Xiangdong Li, Siu-Lan L, Sze-Chung W, Wenzhong, Thornton I (2004) The study of metal contamination in urban soils of Hong-Kong using a GIS-based approach. *Environ Pollut* 129(1):113–124
- Zhang H, Ma D, Die Q, Chen X (1999) An approach to studying heavy metal pollution caused by modern city development in Nanjing, China. *Environ Geol* 38:223–228